Proceedings of the IASS 2024 Symposium
Redefining the Art of Structural Design
August 26-30, 2024, Zurich Switzerland
Philippe Block, Giulia Boller, Catherine DeWolf,
Jacqueline Pauli, Walter Kaufmann (eds.)

Design-to-construction workflow for free-form Abeille stone structures

Yousef Anastas[1]*, Olivier Baverel[2], Maurizio Brocato[3]

[1]*Laboratoire GSA, ENSA Paris-Malaquais, Université PSL, AAU ANASTAS
14 rue Bonaparte, 75006 Paris, France
yousef@aauanastas.com
[2] Laboratoire Navier UMR8205, Ecole des Ponts ParisTech, UGE, CNRS, Champs-sur-Marne, France
[3] Laboratoire GSA, ENSA Paris-Malaquais, Université PSL, Paris, France
14 rue Bonaparte, 75006, Paris, France

Abstract

The paper presents a stone vault built in Jericho, with an innovative construction principle allowing for unforeseen forms for such structures. The architectural innovation stems from structural morphology and stereotomy. The vault is made out of 300 mutually supported stone ashlars. It covers a surface of 60m^2 and spans 7m with a constant thickness of 12cm. The geometry follows the shape of a gyroid surface on which Chebyshev nets set the pattern of the interlocking stones. The formwork has been designed following the structure's shape and ashlars' positioning information as automatically generated files for production. The implemented formwork is a combination of advanced fabrication and local craftsmanship. The workflow includes an interface routine between the geometric and structural definitions. A nonlinear structural model has been developed defining ashlars as linear elastic solids following Mohr-Coulomb criteria.

Keywords: stone, stereotomy, topological interlocking, vault, curved surfaces, ashlars

1. Introduction

The recent interest in stone construction - related to reasons including the sustainable nature of the material – has mainly been informed by one theory described by Hooke in 1678 in the form of an anagram that says: "ut pendet continuum flexibile, sic stabit contigum rigidum inversum" ("As hangs a flexible cable so, inverted, stand the touching pieces of an arch."). [1] This theory implies, as stated in 1966 by Jacques Heyman, that "Stone has no tensile strength". Yet, although the principle set by this theory enables a wide variety of design and construction processes and methods, it also restricts stone structures to a narrow set of possible architectures. Furthermore, the study of stone architectural history reveals that stone has leaned on its bending strength capacities ever since prehistoric times with trilithon typologies [1]. Lintels, architraves, corbelled vaults, are as many archetypal elements of architecture that are associated with stone and that make use of its tensile strength.

In 1699, Joseph Abeille - and later Sébastien Truchet (17th century) - suggested a paradigmatic way of covering a space with a flat ceiling made out of shorter stone elements, called Abeille flat vault [2]. Frezier (in 1737) observed the parallelism with Serlio's wooden floors, in that the particular interweaving of elements adds a bending resistance to the structure [3]. In that regard, Abeille flat vaults can be considered as structures between nexorades as defined by Baverel [4] and traditional vaulting. At the start of the 2000's regained interest in stone architecture led Sakarovitch, Fallacara and Brocato to study Abeille system for curved surfaces [5] [6] [7] [8] [9]. Fallacara introduced a method of applied geometrical transformations to a flat vault to obtain a curved structure [6]. Brocato and Mondardini presented a dome shaped Abeille structure generated through methods used for nexorades [9]. Tessmann

uses the topological interlocking of tetrahedral systems on curved surfaces generating an Abeille structure that is however made of ashlars with non-planar surfaces [10]. More recent methods introduced by Kanel-Belov et al. [11], and Weizmann et al. [12] use the *moving cross-section* procedure that allows for topological interlocking yet not necessarily resulting in completely planar faces of ashlars. Vella and Kotnik use a similar method using non regular tetrahedra with planar surfaces [13].

The following paper presents a complete design-to-construction workflow for Abeille stone structures adapted to free-form surfaces. A parametric model is proposed and validated through a built prototype. The research question that arises is to what extent elemental design, as well as manufacturing, can be coupled to a user-defined structural and constructible free-form Abeille system, and vice versa. The fundamental focus of this paper is referring to an essential principle of stereotomy: the smooth continuity of geometrical and structural information from design to construction.

2. Geometry

Before the establishment of scientific definitions, masonry structures were informed by empirical rules of geometric understanding of the material. The first scientific method is based on thrust networks theorized by Robert Hooke in 1678. Considering static equilibrium, stone voussoirs are simulated through weights applied to a hanging chain. It generates an inverted thrust line that fits into the thickness of an arch. The thrust network method has been developed in the same hanging chain principle but applied to three dimensional shapes [14]. It generates compression only structures. The shapes generated are usually irregular and difficult to panel with regular/rational ashlars. The Abeille system – on which the work in this paper is based – relies on mutually supported stone ashlars, giving the global structure an increased bending resistance through form. As such the global shape chosen for this work is a mathematically defined surface on which it is – a priori- easier to trace known networks for rationalizing the production of stone ashlars.

2.1. Initial geometry

The global form of the vault is a triply periodic minimal surface (TPMS) named gyroid (Figure 1) and that can be approximated through the following equation:

$$\cos(x) \times \sin(y) \ + \ \cos(y) \times \sin(z) \ + \ \cos(z) \times \sin(x) \tag{1}$$
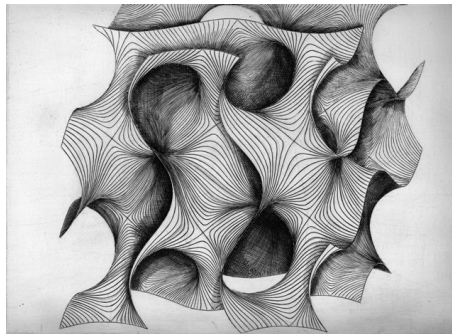

Figure 1 : gyroids representation with curvature lines and asymptotic lines by Patrice Jeener

The initially defined shape is given by defining the domain of *x, y,* and *z* such as:

$$-\frac{\pi}{2} < x < \frac{\pi}{2}; \ \ -\frac{\pi}{2} < y < \frac{\pi}{2}; \ \ -\frac{\pi}{2} < z < \frac{\pi}{2} \tag{2}$$
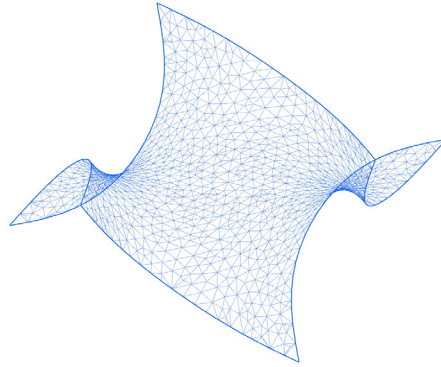
And illustrated below (*Figure 2*):

Figure 2 : Mesh representation of the considered gyroid domain

The mean curvature of a minimal surface is equal to zero at all points. In other words, at any defined point, the radii of principal curvatures are opposite of one another. This allows for form-resistant geometries which the most common example of is the saddle shape. The gyroid form is considered here as the tripod version of the saddle. Using the triply periodic property of the geometry, the global shape is divided into three symmetrical sub-shapes (Figure 3 :).
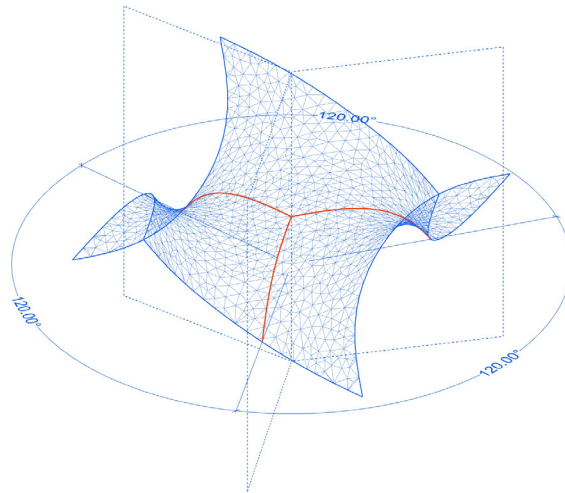

Figure 3 : The gyroid is divided into three symmetrical parts

In the next section a pattern is set on the entire shape with equidistant points. Although this method can be applied to irregular surfaces, the regular properties of the gyroid surface allow for a pattern that is more "homogeneous". It is important to note that the latter property is relevant considering the production of stone ashlars: on irregular surfaces acute angles are more likely to appear, thus weakening the stone voussoirs and resulting in locally concentrated stresses.

2.2. Compass method

The compass method, first proposed by Frei Otto [15] is a geometric method consisting of tracing a grid with equilateral meshes on a target surface. Two arbitrary curves on the surface are chosen having a common intersection point. These two main curves are then divided. The division points are centers of circles that intersect each other. The resulting rose pattern generates an equilateral mesh called Chebyshev net.

In the proposed case, the final mesh geometry is the result of an iterative looping algorithm. To simplify fabrication and construction, the implemented algorithm attempts to approximate the initial surface with a new grid composed of equal-length segments.

Starting from an arbitrary point (in this case the center point of the surface) on the surface, a first sphere centered on the latter point – whose radius equals the length of one side of the net - intersects the surface (*Figure 4*). The intersection results in a curve, called a geodetic (*Figure 4* (a)). This first geodetic curve is divided into a user-chosen number of points. A sphere is then placed at each one of these points and returns geodetic curves on the surface (*Figure 4*(c)). The new collection of points is then found by intersecting with each other the new collection of geodetics.
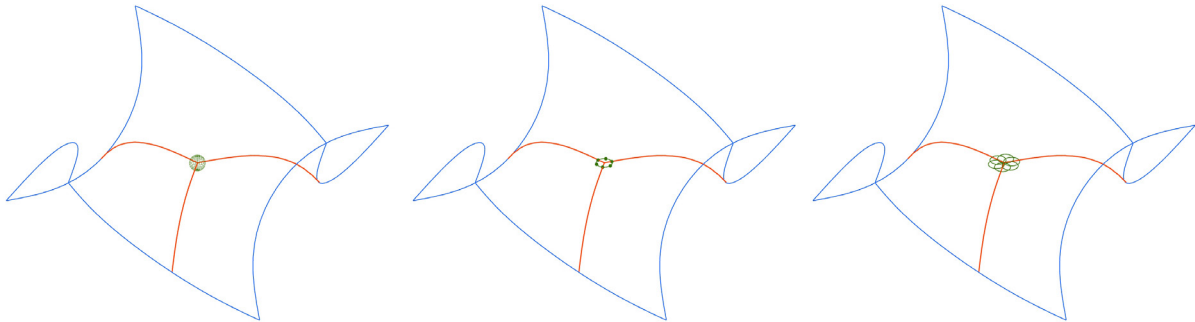

Figure 4: (a) sphere set in the center of the shape. (b) geodetic resulting from the intersection of the sphere with the surface. (c) first generation of geodetic

As the algorithm loops, a rose geometric pattern is created on the whole initial surface, creating a network of equidistant points (Figure 5).
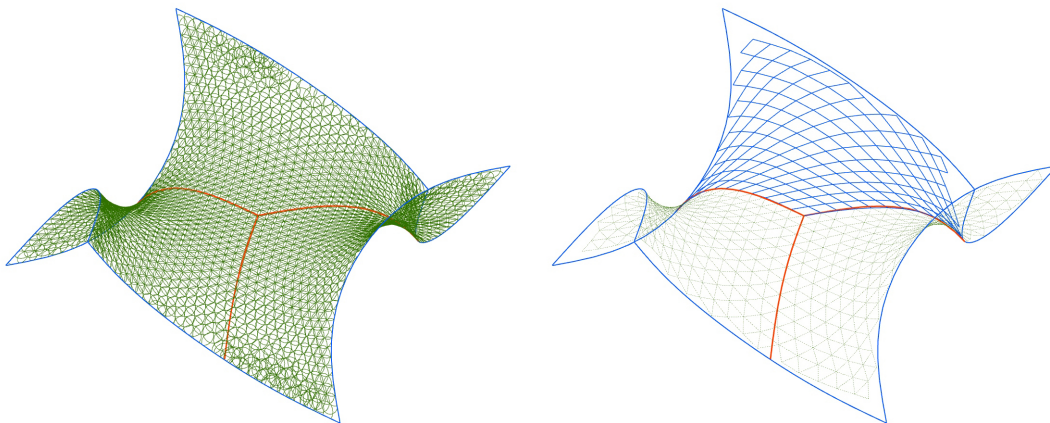

Figure 5: (a) rose pattern of equidistant points on surface. (b) mesh generated by linking equidistant points.

By linking resulting intersection points, a new mesh is generated (Figure 5). The precision (identical length segments) of the generated new grid depends on the initial surface curvature and on the chosen size of module. The more curved the surface in either direction the less precise is the new grid.

The generated mesh is made out of equal-length segments but varying angles. The angle variation allows for a more faithful approximation of the initial shape. The variations are however within an acceptable spectrum thanks to the intrinsic geometrical properties of the minimal surface considered. Figure 5 (b) shows a third of the mesh that will be rotated around the center point to create three identical sub-meshes. It is noticeable on the figure that the edges of the mesh (in blue) are not aligned with the symmetry limits (in orange).

2.3. Geometry adjustment

Once the mesh is generated, a second algorithm is implemented using springs relaxation. The mesh is separated in two parts: springs and nodes. Springs are set to have a rest length equal to the desired segment length, while nodes are left free to move in all directions. The edge nodes are constrained to be pulled to planar curves defining the edge of the surface. The spring relaxation optimization algorithm is used to identify a solution where all spring forces are in a static equilibrium. The mesh shown in *Figure 6* (a) (in blue) is adjusted to the edges set in orange. The final mesh is shown in *Figure 6* (b):
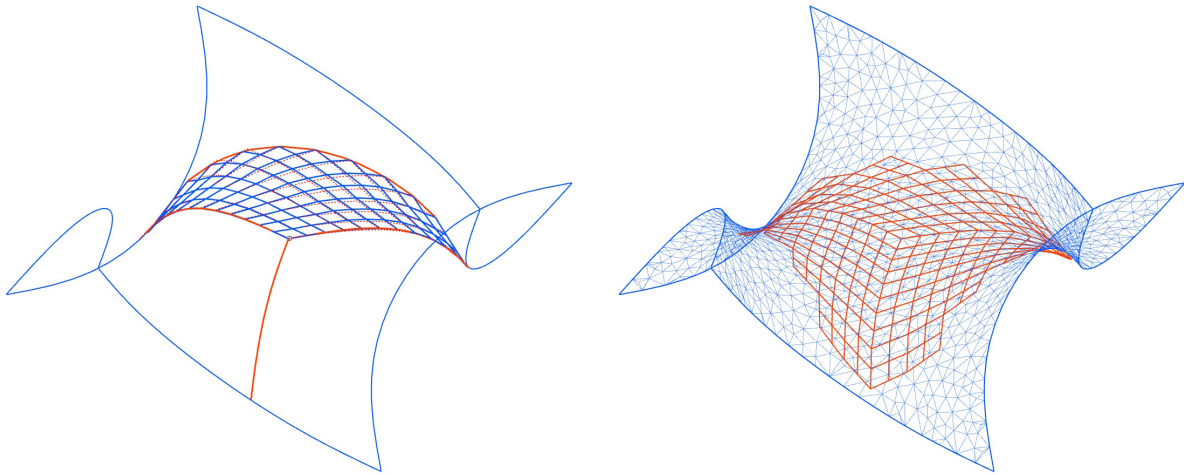
Figure 6: (a) mesh adjusted to edges. (b) final symmetrical mesh

3. Abeille definition on curved surfaces

The following method allows for the generation of curved Abeille structures from Chebyshev nets. The stone voussoirs, also called ashlars, are generated for one third of the structure as shown in Figure 7. In a second phase, the voussoirs are separated into groups related to their position in the structure (edge voussoirs, regular voussoirs, support voussoirs).

3.1. Ashlar generation

The method used for the generation of blocks is described below:

Step 1: the Chebyshev pattern is divided in two groups in a checkerboard fashion (Figure 7).
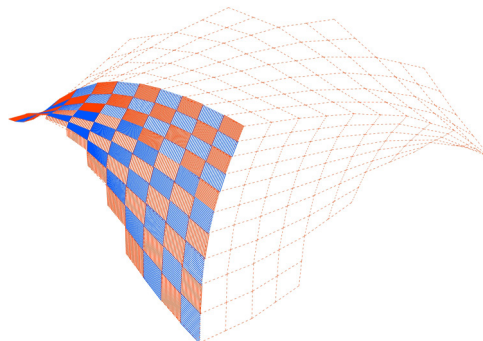
Figure 7 : Checkerboard distribution of mesh pattern. Network A in orange, network B in blue

Step 2: once the quad pattern is separated into two networks (A in orange and B in blue), every segment is named (*a, b, c, d*) as shown in Figure 8. Every cell of network A has a line connecting the center points of segments *a* and *c*. Every cell of network B has a line connecting the center points of segments *b* and *d*.
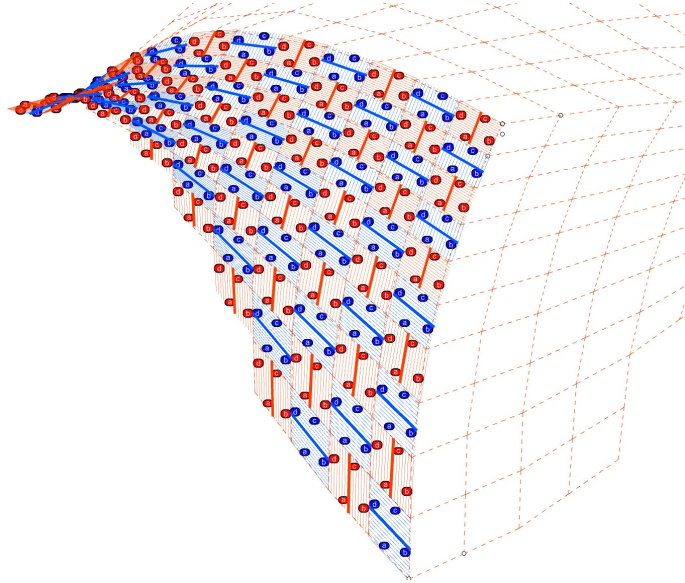

Figure 8: center lines of stone ashlars.

Step 3: for every segment of each network (A and B), a frame is defined such as:

- $\vec{t}$ is the constant tangent vector along each segment represented in cyan color on Figure 9. Vector obtained by calculating the derivative of the position vector with respect to the variable defining its position.
- $\vec{n}$ is the normal vector to the global surface at parameter s of each segment defined as the center point and represented in black on Figure 9
- $\vec{b}$ is the vector perpendicular to the tangent $\vec{t}$ and the principal normal $\vec{n}$. This vector is contained in the normal plane and perpendicular to the osculating plane. Mathematically, the binormal is the result of the cross product between the tangent and the principal normal. It is represented in magenta on Figure 9
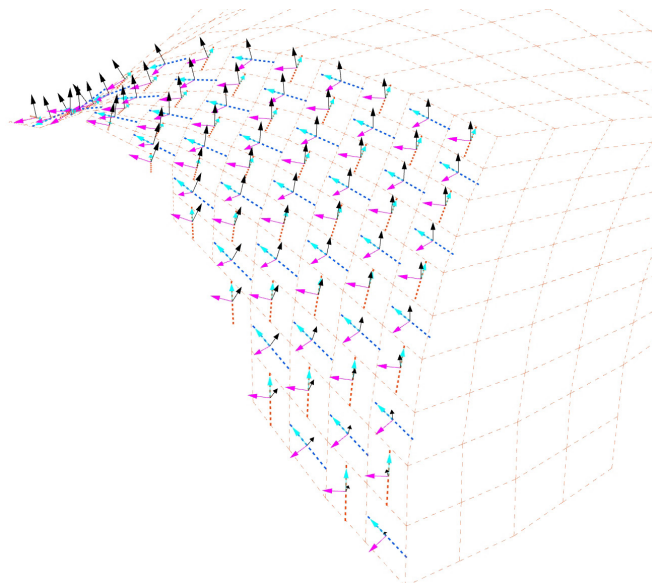

Figure 9: frame definition for ashlars' center lines

<u>Step 4</u>: the initial segments are translated along the binormal vector in two directions with a value corresponding to the lower width of the stone ashlars. The width is set to 12 cm; thus, the segments are translated 6 cm positively and negatively. It has to be noted that the normal vector at parameter *s* as defined previously is not constant along the segments: the global surface being curved, the normal vector varies along the segment. Thus, the binormal vector (being the cross product of the tangent vector and the normal vector) varies as well. Therefore, the translated segments are not coplanar. The polyline shown in Figure 10 is initially not flat.
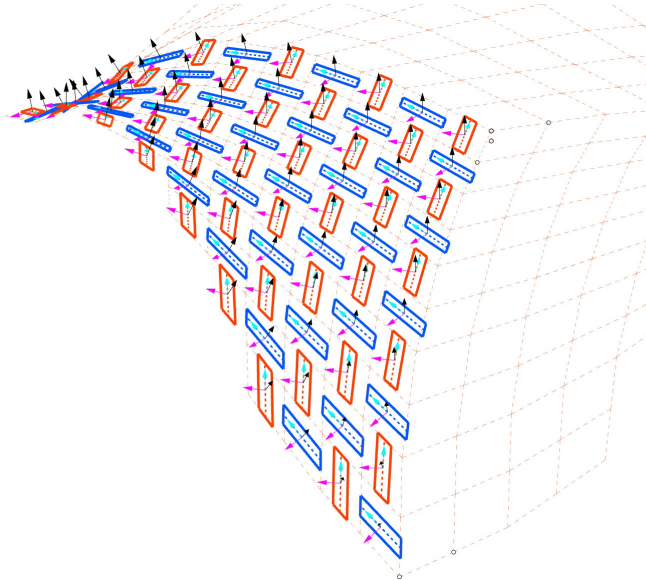

Figure 10: intrados polylines definition

In this paper, a dynamic interactive physical solver tool [16] is used with the following constraints:

- the translated segments have 4 end points (2 for each segment) that are defined as particles linked with length-defined springs. The particles are free to move in space until a solution of planarity is reached.
- the particles are pulled to a surface formed by four points defined as follows:
  - for network A:
    - the two endpoints of the translated segment
    - the two points that are obtained by the intersection of the translated segments and edges *a* and *c* as defined in *Figure 10*
  - for network B:
    - the two endpoints of the translated segment
    - the two points that are obtained by the intersection of the translated segments and edges *b* and *d* as defined in *Figure 10*

Once a solution is reached all polylines of network A and B which are the lower surfaces (intrados) of the vault are flat planar surfaces.

<u>Step 5</u>: planes of each voussoir are defined such as:

- extrados, or upper plane which is defined by translating the planes of the intrados surfaces along the local $\vec{z}$ direction of each plane with a value equal to the defined thickness of stone. The set thickness here is 12cm.
- the long edges planes which are defined by extruding the long edges of the intrados along the local $\vec{z}$ vector of the intrados planes rotated by a set value (*Figure 11*). The value here is equal to 30 degrees and in relation to the coefficient of static friction of the material used.
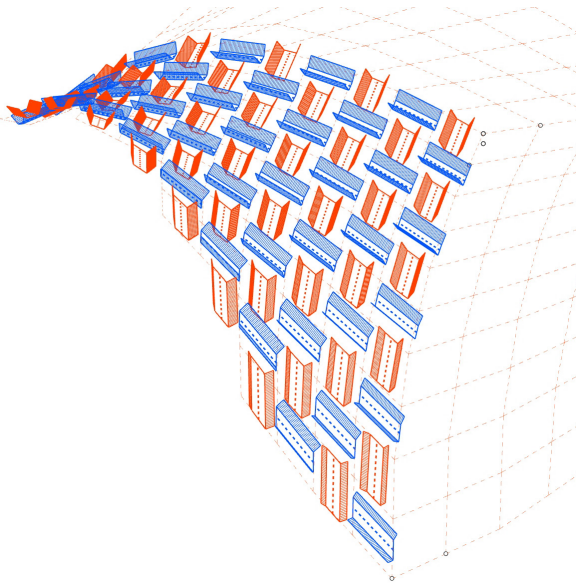
Figure 11: ashlars' long edge planes for both networks

Step 6: the non-hierarchical nature of the structure (Abeille) makes the organization in mutual pairs on a curved surface a problem that is challenging to solve. In the proposed method, an algorithm measures distances between centroids of long-edge surfaces and end points of the defined ashlars. A topological relationship is established between pairs of ashlars. Every voussoir of network A is prolonged to the neighboring voussoirs of network B, and vice versa (Figure 12). The completed structure is shown in *Figure 13*.

Figure 13: Structure completed with all voussoirs

4. Structural analysis

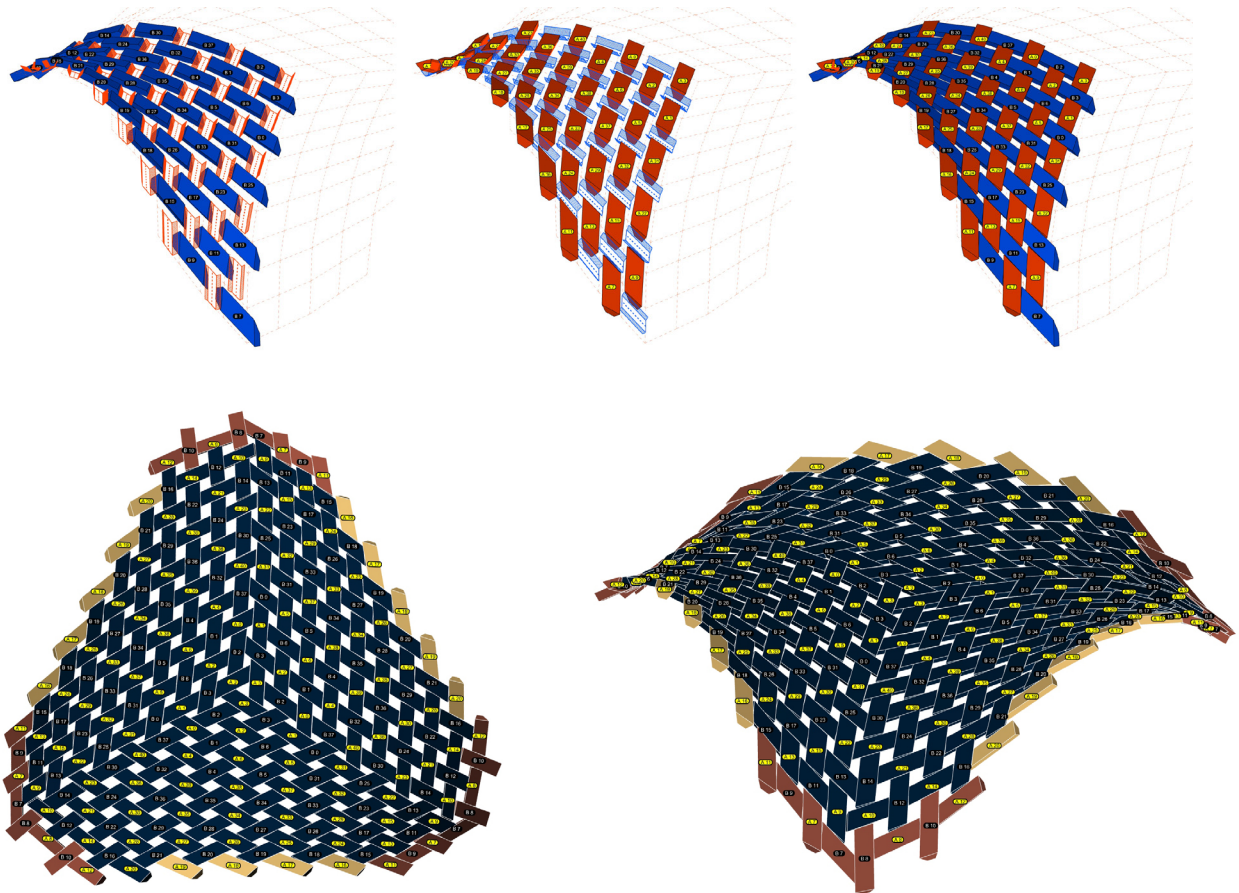The workflow includes an interface routine between the geometric and structural definitions. A nonlinear structural model has been developed defining ashlars as linear elastic heterogeneous solids following Mohr-Coulomb criteria. The finite element mesh is made with a density of 0.045m. The structure is made out of 237 stone voussoirs separated as follows (:

- in green, the regular voussoirs with interfaces modeled as joints with Mohr–Coulomb behavior; joints are considered as dry friction unilateral contact elements (Mohr coulomb model).
- in blue, the support voussoirs which one face is constrained of movements.
- In orange, the edges voussoirs which are attached to the rest of the structure with an epoxy structural glue
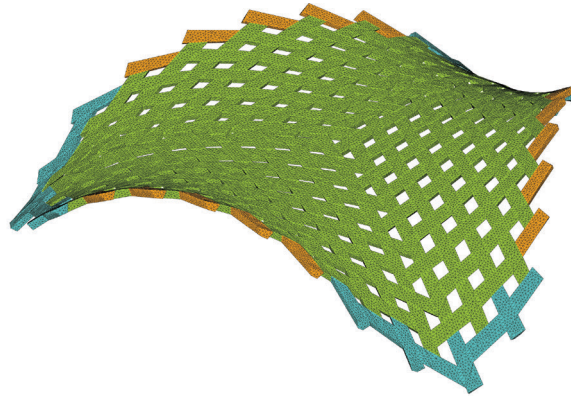

Figure 14: mesh visualization of the structural model

4.1. Materials

4.1.1. Stone

In Palestine, there are two main regions of stone quarries. One in the northern part around Jenin and another in the southern part around Bethlehem and Hebron. At most, every location in the country is less than 50km away from the nearest stone quarry, which also makes the use of the material relevant in terms of carbon footprint. The nature of the material is limestone. The type used for this project is from the region of Bethlehem and is called Injassa, whose properties are given in the following table:

Table 1: Stone material properties

Property	Characteristic value	Standards
Water absorption (%)	1.34	ASTM C 97-09
Bulk specific gravity	2.594	ASTM C 97-09
Compressive strength $\perp$ to rift (Mpa)	123.6	ASTM C 170-09
Compressive strength $\parallel$ to rift (Mpa)	108.9	ASTM C 170-09
Flexural strength$\perp$ to rift (Mpa)	6.53	ASTM C 880-09
Flexural strength $\parallel$ to rift (Mpa)	2.8	ASTM C 880-09
Modulus of elasticity $\perp$ to rift (Mpa)	87887.9	ASTM C 1352-96
Modulus of elasticity $\parallel$ to rift (Mpa)	9751.3	ASTM C 1352-96
Static coefficient of friction	0.86	ASTM C 1028-07

4.1.2. Joints

The stones defined in Figure 14 as edge stones are partially supported by neighboring stones but as well attached to the rest of the structure through a structural epoxy joint with the following properties:

Table 2: joint material properties

Property	Characteristic value
Specific gravity	1.5
Tensile strength (Mpa)	30
Compressive strength (Mpa)	70
Flexural strength (Mpa)	40
Modulus of elasticity in compression (Mpa)	8000
Modulus of elasticity in flexion (Mpa)	4000

4.2. Structural model

4.2.1. Ashlars

Stone ashlars are modelled as linear elastic bodies. The material parameters refer to the material's density (ρ_s), the Young modulus (E_s) and the Poisson ration (υ_s). Actions in the stone are those typical of bending of thick plates. Depending on the location in the vault, part of the stone will be compressed, part tensioned. Stresses within ashlars are limited by three criteria of no fracture based on three measures of the stress state:

- To avoid local failure in compression: the max value of the max principal stress must be smaller than the design compressive strength.
- To avoid local failure in tension: the max abs value of the minimal principal stress must be smaller than the design tensile strength.
- To avoid local failure by excess tangential stress: the max value of the Tresca stress must be smaller than the design tangential strength.

4.2.2. Joints

In the method proposed the geometric topological relation between voussoirs is defined following pairs of neighboring stone voussoirs. In the structural model, edges are built from vertices, faces from edges and volumes from faces. The mesh generated for structural purposes is based on the neighboring criterion defined previously and in order to match nodes and faces of neighboring blocks. Hence, contacts are detected.

4.3. Results

According to Eurocode 6 [17], the static resistance of walls is defined and takes into account the case of a dominating normal stress in the vertical direction. The value is then compared to the design strength. In typical cases, Von mises stress coincides with the normal stress. In the case of a vault, there is no dominant vertical direction. Hence, in accordance with the Eurocode, Von mises is the best way to use an objective measure of the stress state.

Von Mises stress − Max : 2.40180E+07 Pa
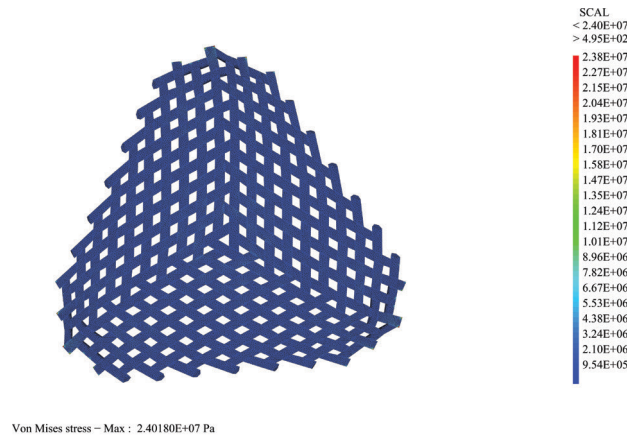
Figure 15: Von Mises stress under dead load

Figure 15 shows a maximum value of Von Mises stress equal to 24Mpa which is to be compared with the compressive design strength defined as follows:

$$f_d = \frac{f_k}{\gamma} = \frac{108.9}{1.5} = 72.6 \, Mpa > 24 Mpa \tag{3}$$

Stresses are evenly distributed in the vault and very low, but more variable on the boundary (*Figure 16*):

Von Mises stress (arcs) − Max : 1.02418E+06 Pa

Figure 16: isolated edge voussoirs Von Mises stress under dead load

A second verification is done with the displacement value. Considering dead load, the displacement along $\vec{z}$ is considered and shown below:

VERTICAL DISPLACEMENTS − MIN : −7.46636E−02 M

Figure 17: vertical displacement under dead load

Maximum displacement is equal to 7 cm which is to be compared with the span design limit of deflection:
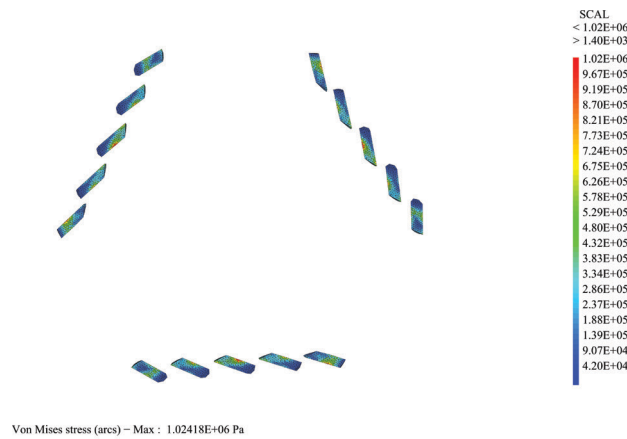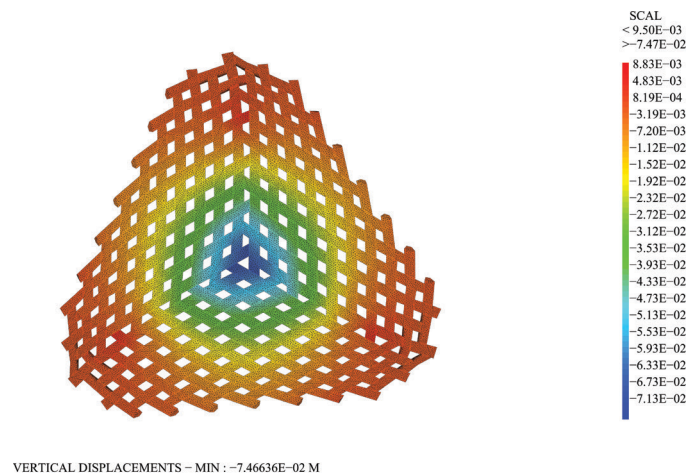
$$\frac{l}{300} = \frac{7}{300} = 0.02m > 0.07m \qquad (4)$$

The calculated deflection exceeds the admissible value. For that reason, the global geometry has been modified to add a camber The central node of the structure has been displaced upwards 10 cm. All other nodes have been accordingly displaced with a parabolic distribution of z values such as:

$$f(x) = -x^2 \qquad (5)$$

with

$$\max \ f(x_{central\ node}) = 0.1m \qquad (6)$$

The entire proposed method has an interface that automatically connects the geometry, fabrication files and structural mesh geometry based on a fully parametric model. As such, it is relatively easy to enable users to do iterations between design and structural analysis to reach an admissible solution. The proposed method also includes an analysis of individual ashlars. This study is important specifically for stone construction. It allows for a better determination of areas of high stress, areas that need to be monitored and eventually areas that might be challenging in terms of production (c.f. acute edges). In the case of the studied project, since the global surface is regular, stresses are fairly even along the ashlars which is a clear advantage in terms of production, mounting and structural behavior.

5. Mounting

5.1. Fabrication

The proposed method includes a generation of files ready for fabrication in different formats (.stl; .dwg; .dxf). All of the stone voussoirs have an identical long edge angle. The small faces are cut with different angles due to the curvature of the overall surface (Figure 18).
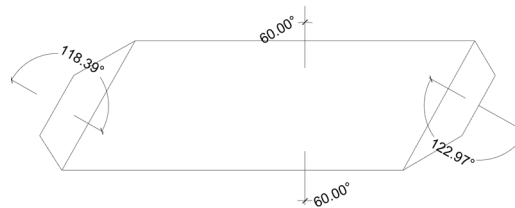
Figure 18: voussoir typology with opposite long edge constant angle and variable small edges angles.

The fabrication process is made using 5 axis cutting machines. Stone blocks are extracted from quarries in dimensions equal to 2.4m long, 1.6m wide and 1.5m high. These blocks are then cut into plates of desired thickness (in this case 12cm). Voussoirs are then cut along their long edge. The small faces are then cut individually (Figure *18*).

Figure 19: 5 axis cutting machine of edge angles

Average weight per voussoirs is 44kg, the lightest being 39kg and the heaviest 47kg. Since the voussoirs are not symmetrical, the method suggests two verification systems to determine the orientation of each voussoir on site:

- Using the edges lengths to verify the voussoir's ID
    - Using individual templates that fit to the "upward" small face of every voussoir.

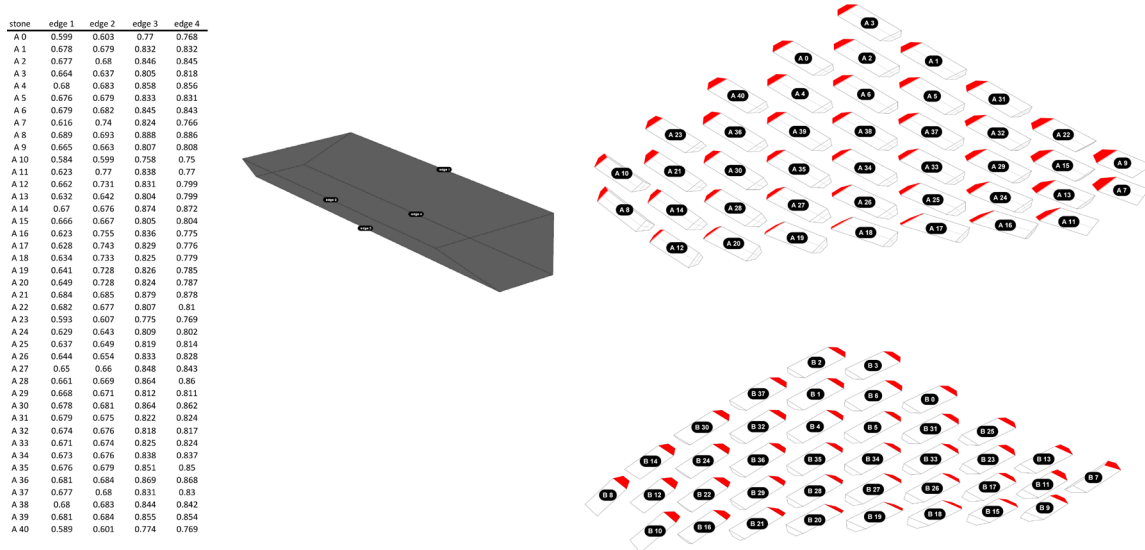| stone	edge 1	edge 2	edge 3	edge 4
A 0	0.599	0.603	0.77	0.768
A 1	0.678	0.679	0.832	0.832
A 2	0.677	0.68	0.846	0.845
A 3	0.664	0.637	0.805	0.818
A 4	0.68	0.683	0.858	0.856
A 5	0.676	0.679	0.833	0.831
A 6	0.679	0.682	0.845	0.843
A 7	0.616	0.74	0.824	0.766
A 8	0.689	0.693	0.888	0.886
A 9	0.665	0.663	0.807	0.808
A 10	0.584	0.599	0.758	0.75
A 11	0.623	0.77	0.838	0.77
A 12	0.662	0.731	0.831	0.799
A 13	0.632	0.642	0.804	0.799
A 14	0.67	0.676	0.874	0.872
A 15	0.666	0.667	0.805	0.804
A 16	0.623	0.755	0.836	0.775
A 17	0.628	0.743	0.829	0.776
A 18	0.634	0.733	0.825	0.779
A 19	0.641	0.728	0.826	0.785
A 20	0.649	0.728	0.824	0.787
A 21	0.684	0.685	0.879	0.878
A 22	0.682	0.677	0.807	0.81
A 23	0.593	0.607	0.775	0.769
A 24	0.629	0.643	0.809	0.802
A 25	0.637	0.649	0.819	0.814
A 26	0.644	0.654	0.833	0.828
A 27	0.65	0.66	0.848	0.843
A 28	0.661	0.669	0.864	0.86
A 29	0.668	0.671	0.812	0.811
A 30	0.678	0.681	0.864	0.862
A 31	0.679	0.675	0.822	0.824
A 32	0.674	0.676	0.818	0.817
A 33	0.671	0.674	0.825	0.824
A 34	0.673	0.676	0.838	0.837
A 35	0.676	0.679	0.851	0.85
A 36	0.681	0.684	0.869	0.868
A 37	0.677	0.68	0.831	0.83
A 38	0.68	0.683	0.844	0.842
A 39	0.681	0.684	0.855	0.854
A 40	0.589	0.601	0.774	0.769

Figure 20: (left) edges lengths verification. (right) templates for voussoirs orientation

5.2. Formwork

The formwork is a hybrid structure made of digitally carved polystyrene blocks and traditional timber construction (Figure 21). The timber formwork is composed of several plywood platforms elevated at different levels to host the polystyrene formwork (*Figure 21* and *Figure 22*) . The use of timber as a base for the formwork minimizes the use of polystyrene blocks.

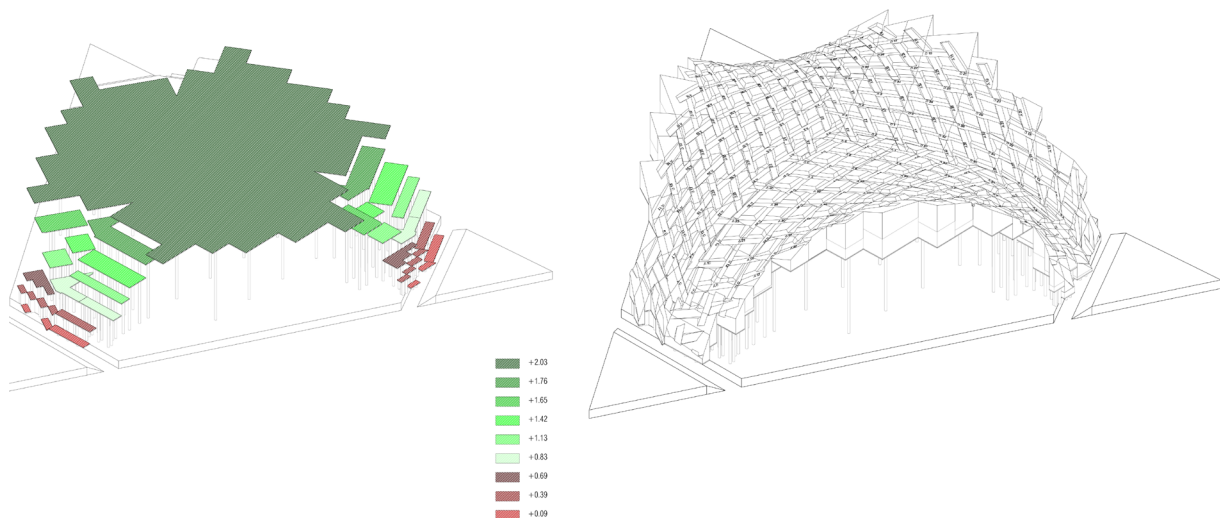
Figure 21: (a) timber formwork with different levels. (b) polystyrene formwork

Figure 22: (left) polystyrene blocks carved. (center)timber formwork and polystyrene blocks. (right) placing of stone voussoirs

The stones are laid on the polystyrene formwork (Figure *22*) starting from the center and concentrically going outwards. Once all the stones are laid, the formwork can be lowered of a few centimeters using the regular steel props.

5.3. Tests

Once the formwork is dissociated from the stone structure, it is left for at least a complete day. Deflection monitoring is done through a dial indicator, a theodolite and some small thin glass panels (Figure 23):

- The dial indicator measures the deflection at the center of the structure
- The theodolite is used as an alternative measuring tool for deflection
- Thin glass panels are fixed to several points on the structure. Any small movement will break the glass.
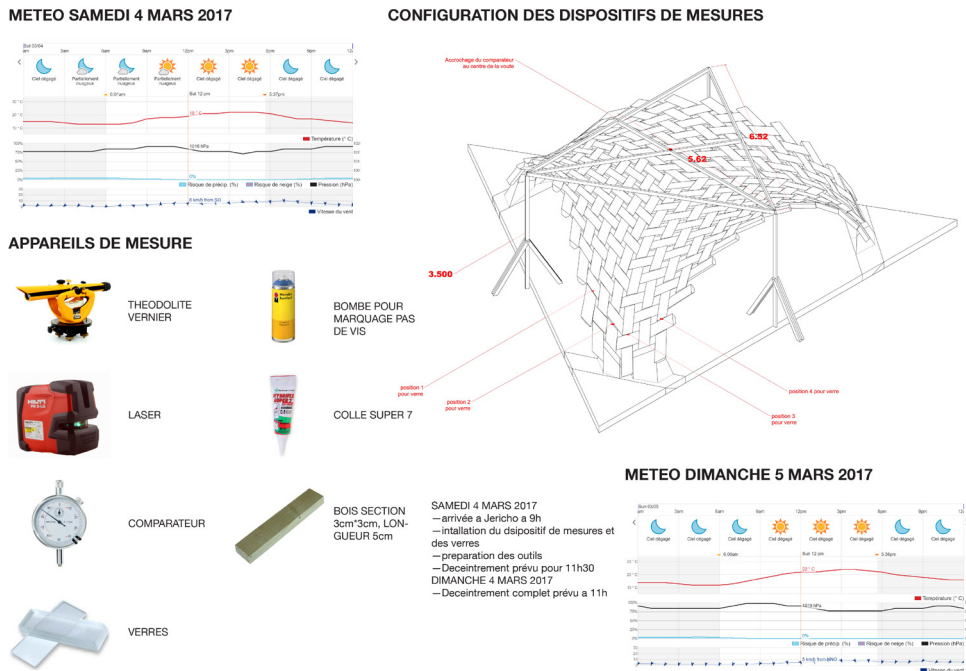

Figure 23: testing and monitoring during un-scaffolding

The theoretical model has been validated through the measured deflection using the dial indicator and the theodolite which have both shown a deflection of 7 cm after complete un-scaffolding (*Figure 24*and *Figure 25*).

Figure 24: completed structure in Jericho after un-scaffolding

Figure 25: completed structure in Jericho after un-scaffolding

6. Conclusion

The paper presents a full methodology – from design to construction – for free-form Abeille structures. The method presented allows for unprecedented shapes for such structures and exposes the advantages of Abeille's hybridity bringing together catenary effects and form bending resistance proper to nexorades. This hybridity allows for even more possible shapes for stone structures. The paper resolves the challenging topological relationships between ashlars in a curved Abeille structure and uses this same neighboring criterion for the definition of the structural model. The paper is above all an attempt at preserving a fundamental principle in stereotomy: ensure the continuity of geometrical and structural information from design to construction. Research explorations remain with regards to linking further knitting and weaved structures models with Abeille inspired structures. The mounting procedure could also be further developed to include formwork-less constructions.

3. Referencing literature

Use the IEEE citation style (more information [here](#)) as shown in the sample reference list at the end of this template. To make it easier for readers to follow reference citations in text, it is recommended that authors refer to previous literature by indicating author names in addition to the numbers in square brackets (e.g. Adriaenssens et al. [1], Chilton [2], or Tibert and Pellgrino [3]). The IEEE style dictates that the references should be numbered and listed at the end of the paper in the order in which they are cited. The reference list should be included at the end of the paper and counts towards the page limits for short and long papers.

Acknowledgements

References

[1] M. Brocato, P. Nougayrede and P. Vergonjeanne, "Tailler, Tasser, Tisser," 2023.

[2] . J.-G. Gallon, Machines et inventions approuvés par l'Académie Royale des Sciences, depuis son établissement jusqu'à present; avec leur description, Paris: Martin-Coignard-Guerin, 1735.

[3] . A.-F. Frezier, La théorie et la pratique de la coupe des pierres et des bois, pour la construction des voûtes et autres parties des bâtiments civils & militaires, ou Traité de stéréotomie à l'usage de l'architecture, Paris: C.-A. Jombert , 1754-1769.

[4] O. Baverel, Nexorade: a family of interwoven space structure, Surrey: University of Surrey, 2000.

[5] R. Etlin, G. Fallacara and L. Tamborero, Plaited Stereotomy. Stone Vaults for the Modern World - Softcover, Rome: Aracne, 2008.

[6] G. Fallacara, "Digital stereotomy and topological transformations : reasoning about shape building," in *Proceedings of the second international congress on construction history. Vol. 1*, Cambridge, 2006.

[7] G. Fallacara, "Toward a stereotomic design: experimental constructions and," in *Third International Congress on Construction History*, cottbus, 2009.

[8] J. Sakarovitch, "Proceedings of the Second International Congress on Construction History," in *Proceedings of the Second International Congress on Construction History* , Queens' College, Cambridge University, 2006.

[9] M. Brocato and L. Mondardini, "Geometric methods and computational mechanics for the design of stone domes based on Abeille's bond," in *Advances in Architectural Geometry* , Vienna, Springer, 2010, pp. 149-162.

[10] O. Tessmann, "Topological interlocking assemblies," in *eCAADe 2012*, Prague, 2012.

[11] A. Kanel-Belov, A. Dyskin, Y. Estrin, E. Pasternak and I. Ivanov-Pogodaev, Interlocking of convex polyhedra : Towards a geometric theory of fragmented solids, arXiv preprint arXiv, 2008.

[12] M. Weizmann, O. Amir and Y. J. Grobman, "Topological interlocking in buildings: A case for the design and construction of floors," *Automation in Construction,* vol. 72, no. part 1, pp. 18-25, 2016.

[13] I. M. Vella and T. Kotnik, "Geometric Versatility of Abeille Vault," in *Proceedings of the 34th International Conference on Education and Research in Computer Aided Architectural Design in Europe (eCAADe) [Volume 2]*, Oulu, 2016.

[14] Thrust network analysis: exploring three-dimensional equilibrium, Boston: Massachusetts Institute of Technology, 2009.

[15] Otto, Frei;, "Grid Shells," *IL,* p. 346, 1974.

[16] D. Picker, "Kangaroo, Live Physics for Rhino and Grasshopper," [Online]. Available: http://kangaroo3d.com. [Accessed 25 August 2015].

[17] Eurocodes, C. E. N, Eurocodes 0-9, BS EN 1990-1999, London : British Standards Institution, 2005.

[18] S. Adriaenssens, P. Block, D. Veenendaal and C. Williams, Shell Structures for Architecture: Form Finding and Optimization, Routledge, 2014.

[19] J. Chilton, "Heinz Isler's Infinite Spectrum: Form-Finding in Desig," *Architectural Design,* vol. 80, no. 4, pp. 64-71, 2010.

[20] A. G. Tibert and S. Pellegrino, "Review of Form-Finding Methods for Tensegrity Structures," *International Journal of Space Structures,* vol. 26, no. 3, pp. 241-255, 2011.

[21] G. Fallacara, "Digital stereotomy and topological transformations reasoning," in *Proceedings of the Second International Congress on construction history*, Queen's College Cambridge, 2006.

[22] M. Brocato and L. Mondardini, "Geometric methods and computational mechanics for the design of stone domes based on Abeille's bond," in *Advances in Architectural Geometry*, Vienna, Springer, 2010, pp. 149-162.